q-exponential relaxation of the expected avalanche size in the coherent noise model

Christopoulos, S-R.G. and Sarlis, N.V.

Original citation & hyperlink:
Christopoulos, S-R.G. and Sarlis, N.V. (2014) q-exponential relaxation of the expected avalanche size in the coherent noise model. Physica A: Statistical Mechanics and its Applications, volume 407 : 216–225
http://dx.doi.org/10.1016/j.physa.2014.03.090

DOI 10.1016/j.physa.2014.03.090
ISSN 0378-4371

Publisher: Elsevier

q-exponential relaxation of the expected avalanche size in the coherent noise model

S.-R. G. Christopoulos, N. V. Sarlis*

Department of Solid State Physics and Solid Earth Physics Institute, Faculty of Physics, School of Science, National and Kapodistrian University of Athens, Panepistimiopolis, Zografos 157 84, Athens, Greece

Abstract

Recently [Phys. Rev. E 85, 051136 (2012)] the threshold distribution function $p_{thres}^{(k)}(x)$ of the coherent noise model for infinite number of agents after the k-th avalanche has been studied as a function of k, and hence natural time. An analytic expression of the expectation value $\mathcal{E}(S_{k+1})$ for the size S_{k+1} of the next avalanche has been obtained in the case that the coherent stresses are exponentially distributed with an average value σ. Here, by using a statistical ensemble of initially identical systems, we investigate the relaxation of the average $\langle \mathcal{E}(S_{k+1}) \rangle$ versus k. For k values smaller than $k_{max}(\sigma, f)$, the numerical results indicate that $\langle \mathcal{E}(S_{k+1}) \rangle$ collapses to the q-exponential [Tsallis, J. Stat. Phys. 52, 479 (1988)] as a function of k. For larger k values, the ensemble average can be effectively described by the time average threshold distribution function obtained by Newman and Sneppen [Phys. Rev. E 54, 6226 (1996)]. An estimate $k_0(\sigma, f)(> k_{max}(\sigma, f))$ of this transition is provided. This ensemble of coherent noise models may be considered as a simple prototype following q-exponential relaxation. The resulting q-values are compatible with those reported in the literature for the coherent noise model.

Keywords: q-exponential, coherent noise model, natural time, off-equilibrium dynamics

*Corresponding author
Email address: nsarlis@phys.uoa.gr (N. V. Sarlis)

1. Introduction

The coherent noise model introduced by Newman and Sneppen[1, 2, 3] is a model that shows reorganization events whose distribution follows a power law over many decades and displays 'aftershock' events. These events have been shown[2, 4] to exhibit a behavior similar to that of the Omori law for real earthquake aftershocks, i.e., they exhibit a power law relaxation. The Omori law describes the temporal decay of aftershock activity and its modified form[5], see also Ref.[6], is given by the relation

$$r(t,m) = \frac{1}{\tau_0 \left[1 + t/c(m)\right]^p}, \tag{1}$$

where $r(t,m)$ the rate of occurrence of aftershocks with magnitudes greater than m per day, t is the time that has elapsed since the mainshock and τ_0 and $c(m)$ are characteristic times. Note that $p \approx 1$ for large earthquakes (e.g., see Ref.[7]). Both real earthquake aftershock sequences as well as coherent noise model aftershocks have been shown[8, 9] to exhibit the aging phenomenon with an associated scaling property which can be described in terms of a scaling function given by the q-exponential appearing in nonextensice statistical mechanics.

Non-extensive statistical mechanics[10] (for a recent review see also Ref.[11]), pioneered by Tsallis[12], is a generalization of Boltzmann-Gibbs statistical mechanics which assumes that the entropy is given by

$$S_q = k \ln_q W \tag{2}$$

where k is the Boltzmann constant, W is the number of discrete states available to the system, q a real number and the q-logarithm is given by

$$\ln_q(x) \equiv \frac{x^{1-q} - 1}{1-q}. \tag{3}$$

Equation (2) for $q \to 1$ reduces to the Boltzmann-Gibbs entropy, $S_{BG} = k \ln W$, because in this case $\ln_q(x) \to \ln(x)$. Nonextensive statistical mechanics provides a consistent theoretical framework for the studies of complex systems in their nonequilibrium stationary states, systems with (multi) fractal and self-similar

structures, long range interacting systems etc (for the various applications see Part III of Ref.[10] and references therein). When considering the arbitrary probabilities $p_i, i = 1, 2, \ldots W$, the Tsallis entropy of Eq.(2) takes the form[10]

$$S_q \equiv k \left(\frac{1 - \sum_{i=1}^{W} p_i^q}{q-1} \right) = -k \sum_{i=1}^{W} p_i^q \ln_q(p_i), \tag{4}$$

which also reduces to the Boltzmann-Gibbs-Shannon entropy $S_{BGS} = -k \sum_{i=1}^{W} p_i \ln(p_i)$ when $q \to 1$. When the discrete states can be labelled by a continuous variable x, p_i's give rise to a probability distribution function $P(x)$ for which the Tsallis entropy is given by

$$S_q \equiv k \left(\frac{1 - \int_0^\infty [P(x)]^q dx}{q-1} \right). \tag{5}$$

The maximization of Eq.(5) under the constraint that the mean value $\langle x \rangle_q$,

$$\langle x \rangle_q \equiv \int_0^\infty x \mathcal{P}(x) dx, \tag{6}$$

where $\mathcal{P}(x)$ is the *escort distribution* defined through[13]

$$\mathcal{P}(x) \equiv \frac{[P(x)]^q}{\int_0^\infty dx' [P(x')]^q}, \tag{7}$$

is known to be $X_q^{(1)}$, i.e., $\langle x \rangle_q = X_q^{(1)}$, leads[10] to the distribution

$$p_{opt}(x) = \frac{\exp_q[-\beta_q^{(1)}(x - X_q^{(1)})]}{\int_0^\infty dx' \exp_q[-\beta_q^{(1)}(x' - X_q^{(1)})]}, \tag{8}$$

where $\beta_q^{(1)}$ is a Lagrange parameter and $\exp_q(x)$ the q-exponential:

$$\exp_q(x) \equiv [1 + (1-q)x]_+^{\frac{1}{1-q}}, \tag{9}$$

where the symbol $[\ldots]_+$ stands for the maximum between 0 and the quantity enclosed by the brackets. When $q \to 1$, Eq.(9) reduces to the Gibbs distribution when x is considered as the energy and then $\beta_q^{(1)}$ is the well known inverse temperature parameter.

The scope of the present paper is to report the appearance of such q-exponential functions when studying an appropriate statistical ensemble based

on the analysis of the coherent noise model. Recently [14], the threshold distribution function $p^{(k)}_{thres}(x)$ of the coherent noise model for the case of infinite number of agents after the k-th avalanche has been studied as a function of k, and hence natural time[15, 16]. Note that an analysis in the natural time domain, which uncovers hidden properties in complex time series[17], has been applied to a variety of fields including seismology (e.g., see Refs.[18, 19]), cardiology[20, 21], physics of complex systems exhibiting self-organized criticality[22], identification of the origin of self-similarity[23, 24], and distinction between similar looking electric signals obeying different dynamics (e.g., see Ref.[25]). In particular, in Ref.[14] an analytic expression of the expectation value $\mathcal{E}(S_{k+1})$ for the size S_{k+1} of the next avalanche has been obtained. Here, by using a statistical ensemble of initially identical systems, we study the behavior of the ensemble average $\langle \mathcal{E}(S_{k+1}) \rangle$ versus k. The numerical results indicate that for k values smaller than some value $k_{max}(\sigma, f)$, $\langle \mathcal{E}(S_{k+1}) \rangle$ collapses to the q-exponential as a function of k. Namely, we have $\langle \mathcal{E}(S_{k+1}) \rangle = \langle \mathcal{E}(S_1) \rangle \exp_q(-k/\tau)$. For larger k values, however, a behavior compatible with the time average threshold distribution found by Newman and Sneppen[1] is recovered.

The paper is organized as follows: Section 2 presents the coherent noise model whereas Section 3 the results. The latter are discussed in Section 4 and summarized in Section 5.

2. The coherent noise model

The avalanches in the coherent noise model result from the following procedure[1, 2]: Consider a system of N_a agents, for each agent i we associate a threshold $x_i, i = 1, 2, \ldots N_a$, that represents the amount of stress that the agent withstands before it breaks. Without loss of generality[1, 2], x_i may come from the uniform distribution in the interval $0 \leq x < 1$. The dynamics of the model consists of two steps, a 'stress' step, which is more important and sufficient to produce large avalanches, and an 'aging' step. During the 'stress' step, we select a random number (or 'stress' level) η from some probability distribution

function $p_{stress}(\eta)$ and replace all x_i that are smaller than η with new values resulting from the uniform distribution in the interval $0 \leq x < 1$. The number of agents whose thresholds are renewed is the size S of the avalanche. During the 'aging' step, a fixed fraction f of agents is selected at random and their thresholds are also replaced with new thresholds resulting again from the uniform distribution in the interval $0 \leq x < 1$. If we assume that $N_a \to \infty$, the thresholds x_i are represented by a threshold distribution function $p_{thres}(x)$ which initially ($k = 0$) is considered uniform in the interval $0 \leq x < 1$, i.e., $p^{(0)}_{thres}(x) = 1$, see Fig.1(a). The size S_1 of the first avalanche ($k = 1$) is just the probability $\text{Prob}[x < \eta_1] = \int_0^{\eta_1} p^{(0)}_{thres}(x)\mathrm{d}x = \eta_1$ which represents the 'mass' of the agents that had thresholds smaller than η_1, see Fig.1(b). After the subsequent 'aging' step (see the orange and brown arrows in Fig.1) the threshold distribution becomes $p^{(1)}_{thres}(x)$, see Fig.1(f). When repeating the two steps for the second time -using η_2- we can obtain S_2 and $p^{(2)}_{thres}(x)$ and so on.

One can show[14] that the threshold distribution $p^{(k)}_{thres}(x)$ after the k-th avalanche is a piecewise constant function having the following general form

$$p^{(k)}_{thres}(x) = \sum_{n=0}^{n_k} d^{(k)}_n \Theta(x - b^{(k)}_n), \tag{10}$$

where n_k is the number of *steps* present in the threshold distribution function after the k-th avalanche and $\Theta(x)$ is the Heaviside (unit) step function, i.e., $\Theta(x) = 0$ if $x < 0$ and $\Theta(x) = 1$ if $x \geq 0$. For example, when $k = 1$, then $n_1 = 1$ with $d^{(1)}_0 = (1 - f)\eta_1 + f$, $b^{(1)}_0 = 0$, $d^{(1)}_1 = 1 - f$ and $b^{(1)}_1 = \eta_1$, see Fig.1(f). Each time a new (random) stress level η_{k+1} is applied, an avalanche of size

$$S_{k+1} = \int_0^{\eta_{k+1}} p^{(k)}_{thres}(x)\mathrm{d}x = \sum_{n=0}^{n_k} d^{(k)}_n(\eta_{k+1} - b^{(k)}_n)\Theta(\eta_{k+1} - b^{(k)}_n), \tag{11}$$

is generated and the real non-negative parameters $b^{(k)}_n$, $d^{(k)}_n$, $n = 0, 1, \ldots n_k$ are updated by the following rules[14]: Let n_{max} be the maximum integer such that

$$b^{(k)}_{n_{max}} < \eta_{k+1} < b^{(k)}_{n_{max}+1}, \tag{12}$$

if $\eta_{k+1} > b^{(k)}_{n_k}$ then $n_{max} = n_k$. Then,

$$b^{(k+1)}_0 = 0 \quad , \quad d^{(k+1)}_0 = (1 - f)S_{k+1} + f,$$

$$
\begin{aligned}
b_1^{(k+1)} = \eta_{k+1} \quad &, \quad d_1^{(k+1)} = (1-f)\left(\sum_{n=0}^{n_{max}} d_n^{(k)}\right), \\
b_2^{(k+1)} = b_{n_{max}+1}^{(k)} \quad &, \quad d_2^{(k+1)} = (1-f) d_{n_{max}+1}^{(k)}, \\
b_3^{(k+1)} = b_{n_{max}+2}^{(k)} \quad &, \quad d_3^{(k+1)} = (1-f) d_{n_{max}+2}^{(k)}, \\
\cdots \quad &, \quad \cdots \\
b_{n_{k+1}}^{(k+1)} = b_{n_k}^{(k)} \quad &, \quad d_{n_{k+1}}^{(k+1)} = (1-f) d_{n_k}^{(k)},
\end{aligned} \tag{13}
$$

where $n_{k+1} = n_k - n_{max} + 1$. Equations (13) are valid as far as η_{k+1} is smaller than unity. If $\eta_{k+1} > 1$, then obviously $S_{k+1} = 1$ and

$$
p_{thres}^{(k+1)}(x) = p_{thres}^{(0)}(x) \tag{14}
$$

with

$$
d_0^{(k+1)} = 1, b_0^{(k+1)} = 0 \tag{15}
$$

and the system has been completely *regenerated*.

Thus, Eq. (10) together with either Eq.(13) or Eq.(14) describe the evolution of the threshold distribution function of the coherent noise model in the case of infinite agents. The evolution of the system as k increases is reflected in the change of the $2n_k$ quantities $b_n^{(k)}, d_n^{(k)}$ for $n = 1, 2, \ldots, n_k$, because $b_0^{(k)} = 0$ and

$$
d_0^{(k)} = 1 - \sum_{n=1}^{n_k} d_n^{(k)}(1 - b_n^{(k)}), \tag{16}
$$

due to the normalization condition of the threshold distribution function $p_{thres}^{(k)}(x)$. The knowledge of the $2n_k$ quantities $b_n^{(k)}, d_n^{(k)}$ for $n = 1, 2, \ldots, n_k$, enables[14] the exact calculation of the probability distribution $p(S_{k+1})$ of the size S_{k+1} of the next avalanche and therefrom the evaluation of the expected avalanche size $\mathcal{E}(S_{k+1})$. In the commonly used[1, 9, 26, 27, 28] case that $p_{stress}(\eta) = \exp(-\eta/\sigma)/\sigma$, the expectation value

$$
\mathcal{E}(S_{k+1}) \equiv \int_0^\infty S_{k+1} p(S_{k+1}) \mathrm{d}S_{k+1} \tag{17}
$$

is given by [14]

$$
\mathcal{E}(S_{k+1}) = \sigma \sum_{l=0}^{n_k} d_l^{(k)} \left[\exp\left(-\frac{b_l^{(k)}}{\sigma}\right) - \exp\left(-\frac{1}{\sigma}\right)\right]. \tag{18}
$$

Equation (18) provides the expected avalanche size for the $k+1$-th avalanche as the system evolves step by step. However, the statistically stationary state -and hence the time averaged behavior that may arise as a competition between the stress step and the aging step- in the coherent noise model has been already studied in Ref.[1]. Newman and Sneppen[1] have evaluated the average threshold distribution $\overline{p}_{thres}(x)$ by balancing the two competing processes and their result leads to

$$\overline{p}_{thres}(x) = \frac{f}{\sigma\left[f + \exp(-x/\sigma)\right] \ln\left\{1 + \frac{f}{1+f}[\exp(1/\sigma) - 1]\right\}}, \tag{19}$$

from which the distribution $\exp(x/\sigma)/\{\sigma[\exp(1/\sigma) - 1]\}$ in the limit $f \to 0$ can be easily extracted. Equation (19) leads[1] to an avalanche size $s(\eta)$ given by

$$s(\eta) = \frac{\ln\left\{1 + \frac{f}{1+f}[\exp(\eta/\sigma) - 1]\right\}}{\ln\left\{1 + \frac{f}{1+f}[\exp(1/\sigma) - 1]\right\}}, \tag{20}$$

when $\eta \leq 1$ and $s(\eta) = 1$ when $\eta > 1$. Accordingly, the resulting expected avalanche size $\mathcal{E}[s(\eta)]$ is given by

$$\mathcal{E}[s(\eta)] = \int_0^\infty \frac{s(\eta)\exp(-\eta/\sigma)}{\sigma} d\eta = \frac{f}{\sigma}\left\{\frac{1}{\ln\left\{1 + \frac{f}{1+f}[\exp(1/\sigma) - 1]\right\}} - \sigma\right\} \tag{21}$$

It is the main scope of the present paper to study how the expected avalanche size of Eq.(18) relaxes to that of Eq.(21) as the number of avalanches k increases when starting from the initial state of the coherent noise model. For this reason, in the next Section, we will study 10^5 simultaneously evolving such models and evaluate the ensemble average $\langle \mathcal{E}(S_{k+1}) \rangle$ after the k-th avalanche.

3. Results

For the purpose of the numerical simulation, we considered 10^5 replicas of the coherent noise model. Each replica started from the initial condition of the coherent noise model ($k = 0$) and its evolution, by means of Eqs.(13) and (14), was studied using the expected size $\mathcal{E}(S_{k+1})$ of Eq.(18) for the first

10^4 avalanches. The ensemble average $\langle \mathcal{E}(S_{k+1}) \rangle$, hereafter also labeled y_k for brevity,

$$y_k \equiv \mathcal{E}(S_{k+1}), \tag{22}$$

is shown in Fig.2 as a function of the number k (of the preceding avalanches) for $\sigma = 0.01$ when f varies from 0 to 5×10^{-3}.

We observe that y_k finally relaxes to the value resulting from Eq.(21) which was found on the basis of the average threshold distribution $\overline{p}_{thres}(x)$ proposed by Newman and Sneppen[1]. The relaxation, however, is obviously non-exponential giving rise to a rather algebraic (power-law like) behavior.

In order to understand this algebraic behavior, we focus on the case when σ is very small, e.g., see Fig.3 where $\sigma = 10^{-4}$, and $f \to 0$. In this case, Eq.(18) simplifies to

$$\mathcal{E}(S_{k+1}) = \sigma \sum_{l=0}^{n_k} d_l^{(k)} \exp\left(-\frac{b_l^{(k)}}{\sigma}\right), \tag{23}$$

where $b_l^{(k)}$ for $l \neq 0$ come from the exponential distribution with average σ and hence $\exp\left(-\frac{b_l^{(k)}}{\sigma}\right) (= u_l^{(k)})$ follow the uniform distribution in the interval [0,1], i.e.,

$$\mathcal{E}(S_{k+1}) = \sigma \left(d_0^{(k)} + \sum_{l=1}^{n_k} d_l^{(k)} u_l^{(k)}\right). \tag{24}$$

When $f \to 0$ the first line of Eq.(13) results in $d_0^{(k)} = S_{k-1}$, where $S_{k-1} \propto \eta_{k-1}$ due to Eq.(11), and hence the term $d_0^{(k)}$ in the parenthesis of Eq.(24) is negligible because η_{k-1} is exponentially distributed with average $\sigma \to 0$. Moreover, using this property recursively starting from the first avalanche, we obtain from Eq.(13) that the only non-vanishing $d_l^{(k)} (= 1 = d_1^{(1)})$ is the one that corresponds to the maximum η_l selected and hence to the minimum $u_l^{(k)}$. Thus, we have

$$\mathcal{E}(S_{k+1}) = \sigma \min\left(u_l^{(k)}, l = 1, 2, \ldots, n_k\right), \tag{25}$$

which in other words means that the ensemble average $\langle \mathcal{E}(S_{k+1}) \rangle$ equals σ times the average of the minimum value obtained out of k uniformly distributed ran-

dom numbers:

$$\begin{aligned}
\frac{\langle \mathcal{E}(S_{k+1})\rangle}{\sigma} &= \int_0^1\int_{U_1}^1\int_{U_1}^1\dots\int_{U_1}^1\int_{U_1}^1 U_1 dU_1 dU_2 dU_3 \dots dU_{k-1} dU_k + \\
&+ \int_{U_2}^1\int_0^1\int_{U_2}^1\dots\int_{U_2}^1\int_{U_2}^1 U_2 dU_1 dU_2 dU_3 \dots dU_{k-1} dU_k + \dots \\
&+ \int_{U_k}^1\int_{U_k}^1\int_{U_k}^1\dots\int_{U_k}^1\int_0^1 U_k dU_1 dU_2 dU_3 \dots dU_{k-1} dU_k = \\
&= k\int_{U_k}^1\int_{U_k}^1\dots\int_{U_k}^1\int_0^1 U_k dU_1 dU_2 \dots dU_{k-1} dU_k \\
&= k\int_0^1 (1-U_k)^{k-1} U_k dU_k \\
&= k\int_0^1 \xi^{k-1}(1-\xi)d\xi = \frac{1}{k+1} \qquad (26)
\end{aligned}$$

The fact that for small σ and f, we have $y_k = \langle \mathcal{E}(S_{k+1})\rangle = \sigma/(k+1)$ prompted us to compare the numerical values plotted in Figs.2 and 3 with the black solid curve that corresponds to $f_k = y_0/(k+1)$, where y_0 is the expected avalanche size before the first avalanche $y_0 = \sigma[1-\exp(-1/\sigma)]$, i.e., Eq.(18) for $n_0 = 0, d_0^{(0)} = 1, b_0^{(0)} = 0$. We see that the lowermost curves in each case almost collapse on f_k strengthening our initial observation that the relaxation follows an algebraic law. Thus, for very small σ and f we expect to have

$$y_k = y_0 \exp_2(-k), \qquad (27)$$

where we made use of the definition of the q-exponential of Eq.(9).

The behavior observed in Figs.2 and 3 together with Eq.(27) prompted us to further investigate the properties of y_k through the ansatz

$$y_k = y_0 \exp_q\left(-\frac{k}{\tau}\right), \qquad (28)$$

where the parameters q and τ were determined -for given values of σ and f- by solving Eq.(28) numerically for y_1 and y_2. In detail, we used the numerical simulation data y_1 and y_2 to solve by the Newton's method the equation

$$2 = \frac{\ln_q\left(\frac{y_2}{y_0}\right)}{\ln_q\left(\frac{y_1}{y_0}\right)} = \frac{\left(\frac{y_2}{y_0}\right)^{1-q} - 1}{\left(\frac{y_1}{y_0}\right)^{1-q} - 1} \qquad (29)$$

that results from the ansazt (28) for the determination of the q value. The τ value was then determined by

$$\tau = -\frac{1}{\ln_q\left(\frac{y_1}{y_0}\right)}, \tag{30}$$

i.e., solving Eq.(28) for $k = 1$. Figure 4 shows some typical examples of the fittings obtained upon using the ansatz of Eq.(28).

4. Discussion

As shown in Fig.4, the proposed ansatz describes well the numerical data before y_k approaches the value of Eq.(21) estimated on the basis of the average threshold distribution $\overline{p}_{thres}(x)$. Figures 2, 3 and 4 indicate that for k values smaller than some value of k labeled $k_{max}(\sigma, f)$, the ensemble average $\langle \mathcal{E}(S_{k+1}) \rangle$ collapses to the q-exponential as a function of k.

It is noteworthy that an estimate $k_0(\sigma, f) (> k_{max}(\sigma, f))$ of this transition can be found when comparing the results of Eqs.(28) with those of Eq.(21). This is so because as we can clearly see from Figs. 2, 3 and 4, y_k begins to deviate from the ansatz of Eq.(28) when k is a few times smaller than the k-value $k_0(\sigma, f)$ at which the curve of Eq.(28) intersects the horizontal line drawn on the basis of Eq.(21), i.e.,

$$y_{k_0(\sigma,f)} = \mathcal{E}[s(\eta)]. \tag{31}$$

Moreover, for k-values a few times larger than $k_0(\sigma, f)$, y_k reaches the value determined by Eq.(21). In other words, $k_0(\sigma, f)$ indicates when the initial q-exponential relaxation ceases and the time averaged behavior described by Eq.(21) takes over. Figure 5 depicts the values of $k_0(\sigma, f)$ obtained as a function of σ for various values of f. We observe that as we decrease σ starting from $\sigma = 1$, and hence more stress steps are allowed before the coherent noise model is regenerated, $k_0(\sigma, f)$ increases following -closely for very small f- the solid line which has been drawn as a guide to the eye. At some value of σ, however, the effect of the aging step described by the parameter f becomes dominant

and $k_0(\sigma, f)$ saturates. The saturation value of $k_0(\sigma, f)$ for the largest f shown, i.e., $f = 5 \times 10^{-3}$, is about a few tens of avalanches, thus the region where a clear q-exponential relaxation can be observed covers approximately the first ten avalanches, e.g., see also Fig.4(c). For larger f values, e.g., for $f = 0.1$ see Fig.6, even the value of y_k for $k \to \infty$ deviates from the time average behavior. This can be understood on the basis of the last line of Eq.(13) where the effect of the largest η_j is attenuated as a geometric progression because $d_{n_{k+1}}^{(k+1)} = (1-f)d_{n_k}^{(k)}$. Thus, large values of f fade away the effect produced by the extreme values of η_j giving rise to a dominant aging step that almost cancels the stress step. In this case, the balancing between the two steps is strongly disturbed and the time average behavior cannot be observed.

From the discussion so far, it becomes clear that the key factor behind the q-exponential relaxation is the stress step, i.e., the value of σ. In order to investigate this hypothesis, we depict in Figure 7 the results obtained from the ansatz of Sec.3 for q and τ in a wide range of the model parameters σ and f. We observe that both values are *practically* independent of f and solely depend on σ, strengthening the conclusion that the stress step is the main origin of the q-exponential relaxation. Fitting these data, we obtained the following expressions for q and τ:

$$q(\sigma) = 2 + 25.60\sigma^2 + 10.83\sigma^4, \tag{32}$$

$$\tau(\sigma) = 1 + 5.42\sigma^{1.12}, \tag{33}$$

which are drawn by solid lines in Figs.7(a) and 7(b), respectively. Equations (32) and (33) have been obtained on the basis of Eq.(27) (e.g., see Fig.3), thus the quantities $q-2$ and $\tau-1$ were fitted by appropriate polynomial and power law functions in each case.

Let us finally compare these q values with those reported in the literature. If we recall that $k_0(\sigma, f)$ should be larger than 10 so that the q-exponential relaxation is clearly observed, Fig.5 shows that Eq.(32) is of practical importance for σ values smaller than approximately 0.25. This is the range in which the

coherent noise model is frequently investigated[1, 9, 26, 27, 28]. As a characteristic example, Tirnakli and Abe [9] investigated aging in coherent noise models in natural time by studying the event correlations and found a non-extensivity parameter $q \approx 2.98$ when $\sigma = 0.2$ (see Fig.5 of Ref.[9]). According to Eq.(32), the value corresponding to $\sigma = 0.2$ is q =3.04 differing only by 2%. As a second example, a recent analysis of return distributions in the coherent noise model[27] has led to q values equal to q =2.0, 2.09, and 2.21 for $\sigma = 0.01, 0.05$ and 0.065, respectively (cf. Fig.1 and Eq.(5) of Ref.[27]). Interestingly, these values lie within 5% compared to those estimated on the basis of Eq.(32).

5. Conclusions

We studied how the ensemble average $\langle \mathcal{E}(S_{k+1}) \rangle$ of the expected avalanche size $\mathcal{E}(S_{k+1})$ relaxes versus the order of the avalanche k in an ensemble of 10^5 coherent noise models starting from their initial state. A q-exponential relaxation is observed during the first avalanches. This is governed by (and mainly due to) the stress step. In this range, we have $\langle \mathcal{E}(S_{k+1}) \rangle = \sigma[1 - \exp(-1/\sigma)] \exp_q(-k/\tau)$, where q and τ solely depend on σ. For larger k values, the ensemble average can be effectively described by the average threshold distribution function obtained by Newman and Sneppen[1]. The obtained q-values are compatible with those found from the analysis of the return distributions in the coherent noise model.

References

[1] M. E. J. Newman, K. Sneppen, Phys. Rev. E 54 (1996) 6226–6231.

[2] K. Sneppen, M. Newman, Physica D 110 (1997) 209 – 222.

[3] M. E. J. Newman, Proc. R. Soc. London B 263 (1996) 1605–1610.

[4] C. Wilke, S. Altmeyer, T. Martinetz, Physica D 120 (1998) 401–417.

[5] T. Utsu, Geophys. Mag. 30 (1961) 521.

[6] R. Shcherbakov, D. L. Turcotte, J. B. Rundle, Geophys. Res. Lett. 31 (2004) L11613.

[7] A. Saichev, D. Sornette, Tectonophysics 431 (2007) 7–13.

[8] S. Abe, N. Suzuki, Physica A 332 (2004) 533–538.

[9] U. Tirnakli, S. Abe, Phys. Rev. E 70 (2004) 056120.

[10] C. Tsallis, Introduction to Nonextensive Statistical Mechanics, Springer, Berlin, 2009.

[11] C. Tsallis, U. Tirnakli, J. Phys.: Conf. Ser. 201 (2010) 012001.

[12] C. Tsallis, J. Stat. Phys. 52 (1988) 479–487.

[13] C. Beck, F. Schlögl, Thermodynamics of Chaotic Systems: An Introduction, Cambridge University Press, Cambridge, England, 1993.

[14] N. V. Sarlis, S.-R. G. Christopoulos, Phys. Rev. E 85 (2012) 051136.

[15] P. A. Varotsos, N. V. Sarlis, E. S. Skordas, Phys. Rev. E 66 (2002) 011902.

[16] P. A. Varotsos, N. V. Sarlis, E. S. Skordas, Natural Time Analysis: The new view of time. Precursory Seismic Electric Signals, Earthquakes and other Complex Time-Series, Springer-Verlag, Berlin Heidelberg, 2011.

[17] S. Abe, N. V. Sarlis, E. S. Skordas, H. K. Tanaka, P. A. Varotsos, Phys. Rev. Lett. 94 (2005) 170601.

[18] N. V. Sarlis, E. S. Skordas, M. S. Lazaridou, P. A. Varotsos, Proc. Japan Acad., Ser. B 84 (2008) 331–343.

[19] N. V. Sarlis, E. S. Skordas, P. A. Varotsos, Phys. Rev. E 82 (2010) 021110.

[20] P. A. Varotsos, N. V. Sarlis, E. S. Skordas, M. S. Lazaridou, Appl. Phys. Lett. 91 (2007) 064106.

[21] N. V. Sarlis, E. S. Skordas, P. A. Varotsos, EPL 87 (2009) 18003.

[22] N. Sarlis, E. Skordas, P. Varotsos, EPL 96 (2011) 28006.

[23] P. A. Varotsos, N. V. Sarlis, E. S. Skordas, H. K. Tanaka, M. S. Lazaridou, Phys. Rev. E 74 (2006) 021123.

[24] N. V. Sarlis, E. S. Skordas, P. A. Varotsos, Phys. Rev. E 80 (2009) 022102.

[25] P. A. Varotsos, N. V. Sarlis, E. S. Skordas, M. S. Lazaridou, J. Appl. Phys. 103 (2008) 014906.

[26] E. Ergun, U. Tirnakli, Eur. Phys. J. B 46 (2005) 377–380.

[27] A. Celikoglu, U. Tirnakli, S. M. D. Queirós, Phys. Rev. E 82 (2010) 021124.

[28] A. Celikoglu, U. Tirnakli, Physica A 392 (2013) 4543 – 4548.

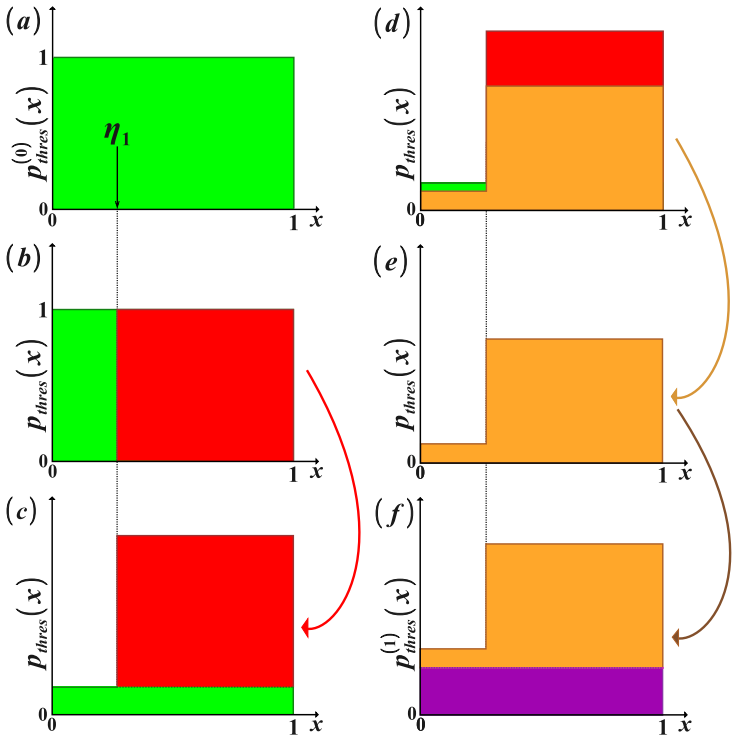

Figure 1: (color online) Construction of the threshold distribution $p^{(1)}_{thres}(x)$ after the first avalanche in the coherent noise model when $N_a \to \infty$: (a) the initial (uniform) distribution function $p^{(0)}_{thres}(x)$. Stress step (shown by the red arrow): (b) Application of the first stress level η_1 (the size S_1 of the first avalanche corresponds to the green shaded area), and (c) a probability mass equal to S_1 is uniformly distributed in the region [0,1]. Aging step (shown by orange and brown arrows): (d) the threshold distribution in (c) is reduced by a fraction f, see panel (e), and a probability mass f is distributed uniformly in the region [0,1] in order to obtain the threshold distribution $p^{(1)}_{thres}(x)$ after the first avalanche which is shown in panel (f).

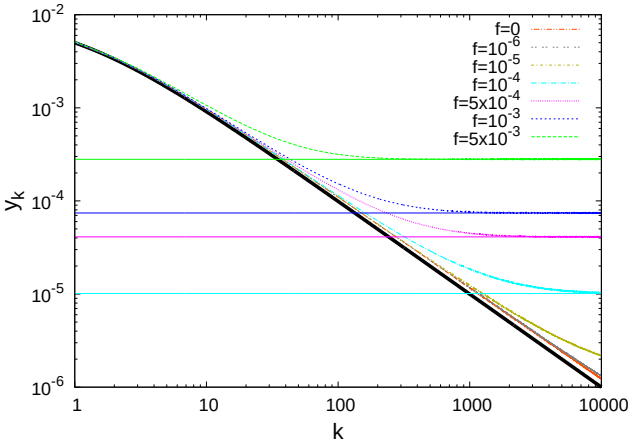

Figure 2: (color online) The ensemble average $\langle \mathcal{E}(S_{k+1}) \rangle$, herafter labeled y_k as a function of the number k of the preceding avalanches for $\sigma = 0.01$ and $f = 0, 10^{-7}, 10^{-6}, 10^{-5}, 10^{-4}, 5 \times 10^{-4}, 10^{-3}$, and 5×10^{-3}. The horizontal solid lines indicate the values obtained from Eq.(21) for $f = 10^{-4}, 5 \times 10^{-4}, 10^{-3}$, 5×10^{-3} and are drawn with the corresponding colors. The thick black solid curve corresponds to $f_k = \sigma[1 - \exp(-1/\sigma)]/(k+1)$.

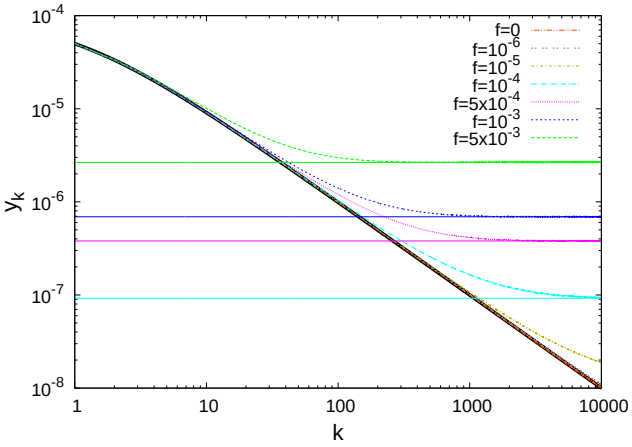

Figure 3: (color online) The same as Fig.2 but for $\sigma = 10^{-4}$.

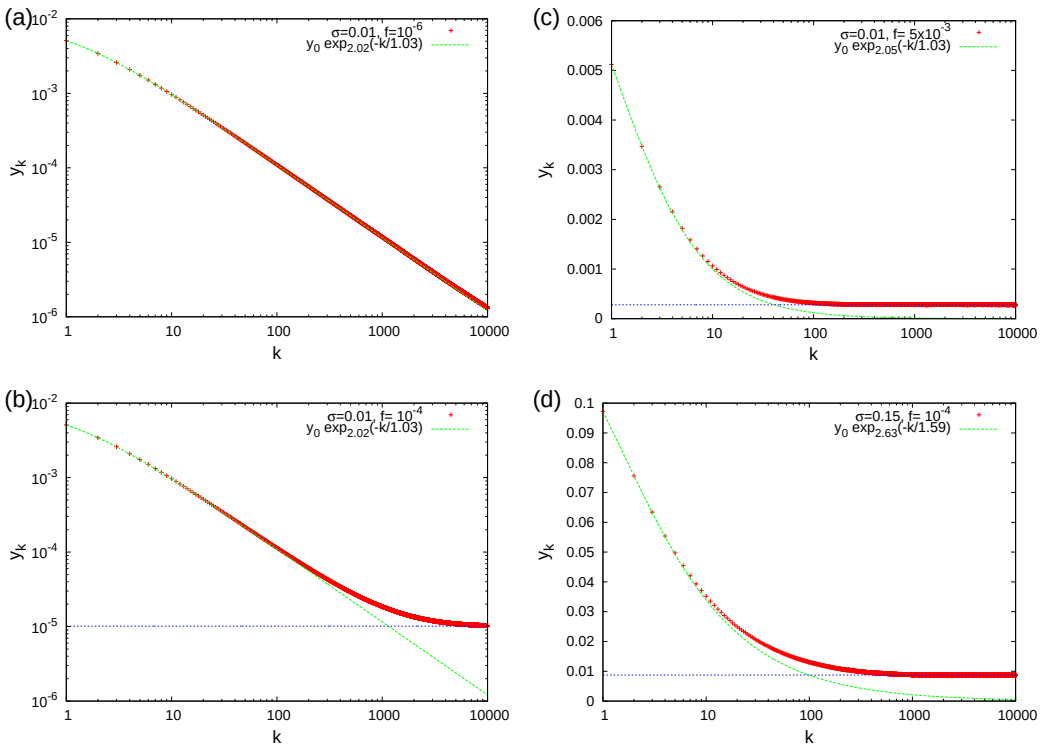

Figure 4: (color online) Indicative examples of fitting the numerical data by the ansatz of Eq.(28) (green dashed curve) for various values of σ and f: (a) $\sigma = 0.01, f = 10^{-6}$, (b) $\sigma = 0.01, f = 10^{-4}$, (c) $\sigma = 0.01, f = 5 \times 10^{3}$ and (d) $\sigma = 0.15, f = 10^{-4}$. The horizontal lines result from Eq.(21).

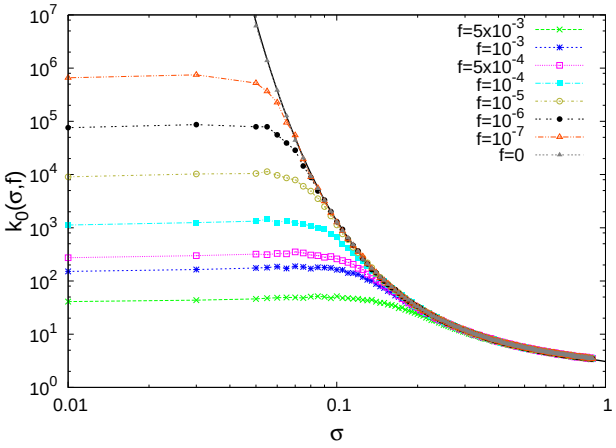

Figure 5: (color online) The estimate $k_0(\sigma, f)$ as a function of σ for various values of f. The thick solid line corresponds to $6.17\sigma^2[\exp(1/\sigma) - 1.39][1 - \exp(-0.468/\sigma)]$ and has been drawn as a guide to the eye.

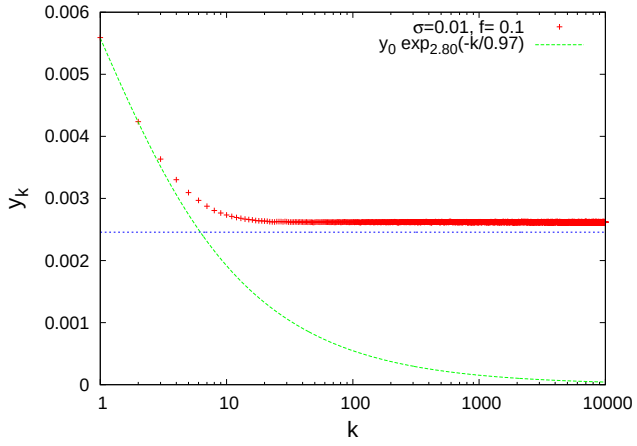

Figure 6: (color online) The same as Fig.4, but for $\sigma = 0.01$ and $f = 0.1$.

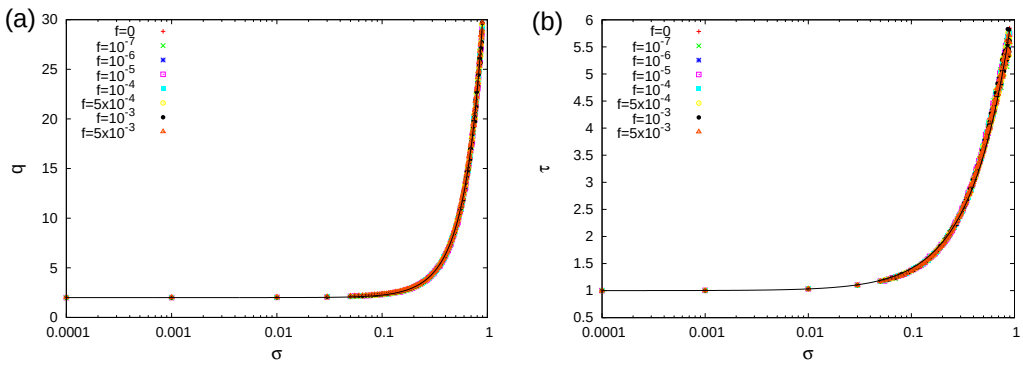

Figure 7: (color online) The estimated ansatz parameters (a) q and (b) τ of Eq.(28) versus σ for various f values in the range $[0, 5 \times 10^{-3}]$, the solid lines correspond to Eqs.(32) and (33), respectively.